VERSITA

# NUMERICAL STUDY OF THE SIZE OF REPRESENTATIVE VOLUME ELEMENT FOR LINEAR ELASTICITY PROBLEM

ADRIAN RÓŻAŃSKI, DARIUSZ ŁYDŻBA

Institute of Geotechnics and Hydrotechnics, Wrocław University of Technology,
WybrzeżeWyspiańskiego 27, 50-370 Wrocław, Poland.
E-mail: adrian.rozanski@pwr.wroc.pl; dariusz.lydzba@pwr.wroc.pl

PIOTR JABŁOŃSKI

5th year student of Wrocław University of Technology, Faculty of Civil Engineering.

**Abstract:** In the paper, a numerical study of the size of representative volume element for the linear elasticity problem is performed. The calculations are carried out for three different types of random microstructures: checkerboard, the Ising model microstructure and Debye microstructure. It is postulated and then verified that there exists a relation between the morphology of microstructure contained in the lineal-path function and the minimum RVE size. It is confirmed, on the basis of numerical examples, that for all the microstructures considered the largest lineal-path can be treated as the size of RVE.

## 1. INTRODUCTION

A sample of random heterogeneous material can be treated as a realization of a certain random or stochastic process. A realization is an event, say $\omega$, and it belongs to a sample space, $\Omega$. Then, the ensemble is regarded as a collection of all possible realizations of a random medium generated by a certain random or stochastic process. The composite media are usually assumed to be statistically homogeneous and therefore these realizations are different in view of the microscopic scale, while from the "macroscopic details" point of view the realizations are identical [1], [19]. Any particular random medium property, say $\xi(\mathbf{x}; \omega)$, is a function of space position $\mathbf{x}$ and realization $\omega$. An ensemble average of $\xi$, at a given localization $\mathbf{x}$, is defined as

$$\overline{\xi(\mathbf{x})} = \int_{\Omega} \xi(\mathbf{x}; \omega) p(\omega) d\omega , \qquad (1)$$

where $p(\omega)$ is the probability density function of $\omega$ in $\Omega$. One can remark that the ensemble average (1) is equivalent to an expectation of the function $\xi(\mathbf{x}; \omega)$. Furthermore, with the assumption of statistical homogeneity of the medium, the ensemble average (1) does not depend on the space variable $\mathbf{x}$.

According to definition (1), one can easily observe that determination of ensemble average of $\xi(\mathbf{x}; \omega)$ requires generation of all the realizations forming ensemble, then evaluation of $\xi(\mathbf{x}; \omega)$ for each realization $\omega$, and finally, averaging over all realizations. This cumbersome procedure causes that it is meaningful to introduce the ergodic hypothesis which allows the ensemble averaging to be replaced with volume averaging providing that the volume tends to infinity

$$\overline{\langle \xi \rangle} = \langle \xi \rangle = \lim_{V \to \infty} \frac{1}{V} \int_V \xi(\mathbf{x} + \mathbf{y}) d\mathbf{y} \,. \qquad (2)$$

Relation (2) gives the possibility of considering only one arbitrary realization providing that the sample volume is infinite. The term "a sample of infinite volume" means, in engineering applications, a sufficiently large sample. This sufficiently large sample is referred to as the representative volume element (RVE) and is usually regarded as a volume of heterogeneous body which is small enough from a macroscopic point of view and simultaneously large enough to contain a sufficient number of inhomogeneities.

In the literature, a large number of specific RVE definitions can be found [3], [20]. These definitions are usually mathematically strict, however, none of them provides precise information on the size of RVE – they do not quantify the size of RVE. Hence, a separate problem is the determination of the size of RVE. Numerous attempts have been made in order to quantify the size of RVE on the basis of both statistical and numerical analyses [6], [20], [3], [5]. Some methods taking into account microstructural statistics as well as microstructure morphology have been formulated in [4], [12], [24], [8].

In this paper, a methodology developed and presented in a series of authors' works [14]–[17] is adopted for an estimation of the ensemble average (1) or (2). According to previous ([14]–[17]) considerations the sample is treated as a set of a finite number $n$ of RVE elements (Fig. 1). Each element has the same finite size $N_{RVE}$. As previously, the problem concerns digital images of microstructure, and hence, $N_{RVE}$ is understood here as the number of pixels in a row/column of a square digital image.
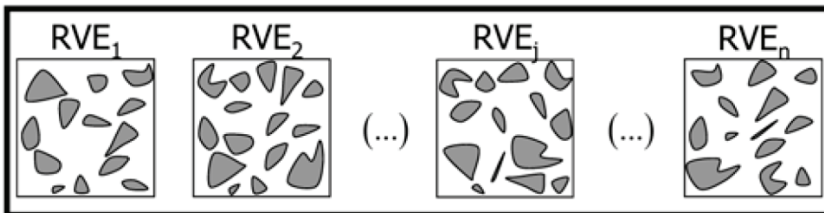


Fig. 1. Graphical illustration of the notion of the sample

The ensemble average is then estimated as

$$\overline{\langle \xi \rangle} \approx n^{-1} \sum_{j=1}^{n} \langle \xi_j \rangle = n^{-1} \sum_{j=1}^{n} \frac{1}{V_{RVE}} \int_V \xi_j(\mathbf{y}) d\mathbf{y} \qquad (3)$$

where $\xi_j$ is a function corresponding to the *j*-th random realization of RVE while *n* is the size of the sample. Within this approach the primary role is played by the proper evaluation of the RVE size as well as the sample size *n*. Note that both values, i.e., $N_{RVE}$ and *n* are related to each other – the larger (smaller) the size of RVE, the smaller (larger) the sample size can be used. Furthermore, it has to be strongly emphasized that the size of RVE cannot be arbitrary. In other words, the chosen RVE size cannot be as small as one may wish. It can be shown that there exists a certain minimum size of RVE which cannot be decreased in order to obtain a proper estimation of the ensemble average. As was demonstrated (see, e.g., [14], [17], [15]) for the case of a heat flow problem, the use of RVE smaller than the minimum one usually results in the overestimation of the effective thermal conductivity coefficient. The same conclusion has also been stated by Kanit [8] for linear elasticity problem.

This paper deals mainly with the problem of numerically efficient evaluation of the RVE size, $N_{RVE}$, for the linear elasticity problem. In the literature, the size of RVE is usually proposed to be determined by investigating the convergence of apparent properties with increasing the size of RVE. Such algorithms usually require a very large number of numerical calculations, e.g., FE analysis. Therefore, in this work, some numerical studies are performed in order to investigate the convergence of apparent elastic properties as well as to search for the relation between the RVE size and the microstructural descriptor, namely the lineal-path function. If there exists some relation between these quantities, then the cumbersome procedures of RVE size evaluation could be overcome. It would appear then that determination of RVE size does not require a large number of numerical simulations, only the morphology of microstructure (contained in the lineal-path) has to be known.

Numerical studies are performed for three different digital images of random microstructures. Each microstructure is a two-phase composite, whose constituents are assumed to be isotropic. As a prelude for further works only one value of contrast in mechanical properties is considered. It is assumed that the ratio of elastic constants is 1 : 10, i.e., $\lambda_1/\lambda_2 = G_1/G_2 = 1/10$. The symbols $\lambda_i$ and $G_i$ are Lame's constants for phase *i*.

The paper is organized as follows. In Section 2, digital images as well as reconstruction procedures of all the random microstructures considered are presented. Next, a microstructural descriptor used in the study, namely the lineal-path function, is briefly described. Graphical presentation of the aforementioned microstructural measure is also provided. Section 4 contains the results of numerical studies. Final conclusions end the paper.

## 2. RANDOM MICROSTRUCTURES

Three types of two-phase random microstructures are considered. A common feature of these microstructures is an equal volume fraction of constituents, i.e., $\phi_1 = \phi_2 = 0.5$. In the following, numerical procedures for microstructure generation are briefly described.

### 2.1. RANDOM CHECKERBOARD

A random checkerboard is easily constructed by first tessellating a unit square into smaller ones (pixels). Then, numerical reconstruction is as follows: pseudo-random number uniformly distributed in the range 0 to 1 is generated for each pixel. Next, if the random number is less than the assumed value of probability $p$, the pixel is filled with black color, otherwise white color is assigned. A digital image of the reconstructed realization is presented in Fig. 2.
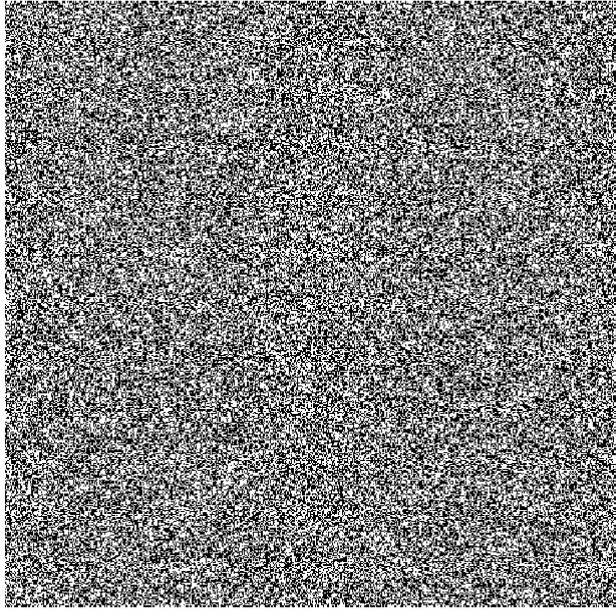


Fig. 2. A digital image (500 × 500 pixels) of the reconstructed 2D realization
of random checkerboard; $p = 0.5$

Since the microstructure is characterized by the equal volume fractions of constituents, therefore the one presented in Fig. 2 was generated with the probability $p = 0.5$. Furthermore, for clarity, white pixels are treated as phase 1, whereas the black ones

are defined as phase 2. It should also be mentioned that throughout this work all pseudo-random numbers are generated using the Marsaglia–Zaman generator that is a part of Mathematica software [11]. More details concerning the Marsaglia–Zaman and other generators as well as their quality checks can be found in [7].

<center>2.2. THE ISING MODEL MICROSTRUCTURE</center>

The Ising model has been originally formulated to model a spontaneous magnetization of ferromagnet in the absence of an external field. This model considers an idealized system of interacting particles arranged on a regular, planar grid. Only one of two magnetic spin orientations can be prescribed to each particle, generally labeled up (+1) and down (–1). The general assumption of the model considered is that each particle interacts only with its nearest neighbors.

Roughly speaking, the procedure of microstructure generation consists in assigning two possible states to each pixel: –1 or +1. Then, we draw one pixel from all pixels contained in the digital image. For the chosen pixel the change of state is proposed, i.e., if the pixel has the +1 (–1) state the change into –1 (+1) is suggested. The new value, –1 or +1, is then accepted with certain probability $p$ defined within the model. The acceptance consists in generating a uniformly distributed random number $u \in [0, 1]$ – if $u < p$ the change of state is accepted, otherwise the value assigned to the pixel is not changed. The microstructure obtained by the Ising model is presented in Fig. 3.
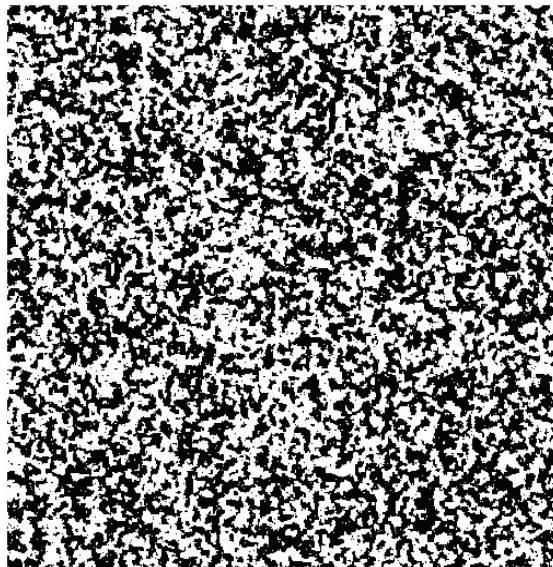


Fig. 3. A digital image (500 × 500 pixels) of microstructure generated via the Ising model

## 2.3. DEBYE MICROSTRUCTURE

Debye microstructure was obtained by making use of reconstruction procedure based on the two-point correlation function. An algorithm was presented in the authors' previous paper [16], where the reconstructed 2D realization of the B$_4$C/Al composite was considered. For more theoretical background, the reader is referred to [22] and [23].

Roughly speaking, the process of reconstruction consists in finding such a realization for which the calculated two-point correlation function matches best the "target" two-point correlation function. The "target" function can be established, e.g., in the way of laboratory investigations or theoretical models. Note that the two-point correlation function is a microstructural descriptor that is widely used by scientists for different purposes (see, e.g., [21]). In the case of both statistically homogeneous and isotropic media the two-point correlation function for phase $i$, $S_2^{(i)}$, is the probability that two ends of a line segment of length $r$ lie in phase $i$ when randomly placed in the sample.

In the case of the Debye random medium the "target" two-point correlation function is as follows

$$\widetilde{S}_2^{(1)}(r) = \phi_1 \phi_2 \exp(-r/a) + \phi_1^2 . \tag{4}$$

Reconstruction process begins with the initial configuration in the random checkerboard arrangement. Then the microstructure is evolved towards $\widetilde{S}_2^{(1)}$ by minimizing the energy $E$, which at any time step is defined as

$$E = \sum_r [\widetilde{S}_2^{(1)}(r) - S_2^{(1)}(r)]^2 \tag{5}$$

where $S_2^{(1)}$ is the two-point correlation function for phase 1 calculated at any time step. The minimization of $E$, at any time step, is performed by simulated annealing algorithm [9], i.e., the states of two arbitrarily chosen pixels of different phases are interchanged – white pixel is changed into black one, while black pixel is filled with white color. Interchanging the states of two pixels causes the change in energy, such that $E \rightarrow \overline{E}$ . Therefore, the difference between two states can be calculated as

$$\Delta E = \overline{E} - E . \tag{6}$$

Then the phase interchange is accepted with some probability

$$p_{\Delta E} = \begin{cases} 1, & \Delta E \leq 0, \\ \exp(-\Delta E / T), & \Delta E > 0, \end{cases} \tag{7}$$

where $T$ is the fictitious temperature and its actual value is defined by the cooling schedule procedure applied. The solution is obtained as $T \rightarrow 0$.
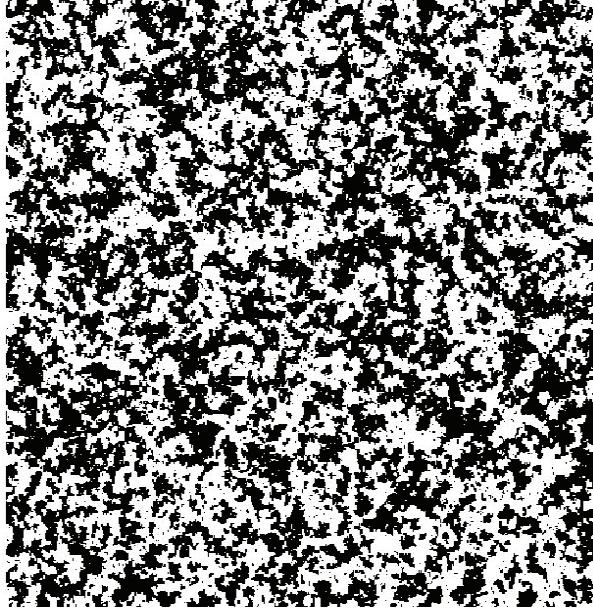
Fig. 4. A digital image (500 × 500 pixels) of the reconstructed 2D realization
of the Debye random medium; *a* = 3

## 3. LINEAL-PATH FUNCTION

Lineal-path function is a microstructure descriptor which statistically describes the microstructure [10]. In what follows, a brief presentation of this microstructure descriptor is provided. Nevertheless, more details as well as applications of the lineal-path function can be found in the works of Quintanilla and Torquato [13], and Yeong and Torquato [22], [23].

In the case of statistically isotropic media, the lineal-path function for phase *i*, $L^{(i)}(r)$, is the probability that a line segment of length *r* lies wholly in phase *i* when randomly "thrown" into the sample. Thus, the lineal-path function contains a higher level of connectedness information than the aforementioned two-point probability function. This is due to the fact that the latter concerns only two end points of the line segment.

The lineal-path function, $L^{(i)}(r)$, is a monotonically decreasing function of *r* and the following limiting values exist

$$L^{(i)}(0) = \phi_i \quad \text{and} \quad L^{(i)}(\infty) = 0 . \tag{8}$$

Furthermore, the lineal-path function denotes the value of probability, and therefore it is evident that for two-phase media

$$L^{(1)}(r) + L^{(12)}(r) + L^{(2)}(r) = 1 \qquad (9)$$

where $L^{(12)}(r)$ is the probability that a line segment of length $r$ lies wholly in two phases simultaneously. In other words, it is a probability that a line segment of length $r$ intersects the interface between two phases when randomly placed in the microstructure.

The values of lineal-path function (for both phases), for all three microstructures presented in the previous section, were determined and are graphically presented in Figs. 5 through 7. Note that, for a given phase, the lineal-path function was evaluated by simple Monte Carlo simulations, i.e., a line segment of length $r$ was randomly placed in the digital image of microstructure and successful hits (the whole line lies in phase $i$) were counted and divided by the total number of throws according to the following expression

$$L^{(i)}(r) = \frac{n_s(r)}{n_T} \qquad (10)$$

where $n_s(r)$ is the number of successful hits and $n_T$ denotes the total number of throws.

Observing the plots (Figs. 5–7) we see that phase connectedness is exhibited by the "tail" of the lineal-path function which gives the information about the largest lineal-paths in phase $i$. The largest path is observed for Debye microstructure, whereas the shortest one for random checkerboard. Moreover, for all three microstructures the lineal-path function shows that the connectedness of both phases is approximately on the same level, i.e., for all values of $r$ $L^{(1)}(r) \approx L^{(2)}(r)$. This is due to fact that these microstructures are of polycrystalline type, i.e., one cannot distinguish in the morphology of the microstructure between the matrix and the inclusion.
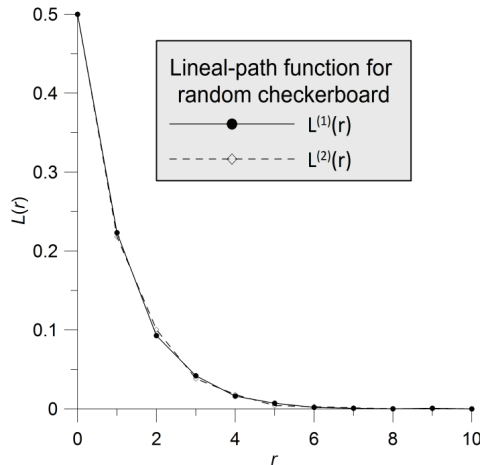


Fig. 5. Lineal-path function for random checkerboard
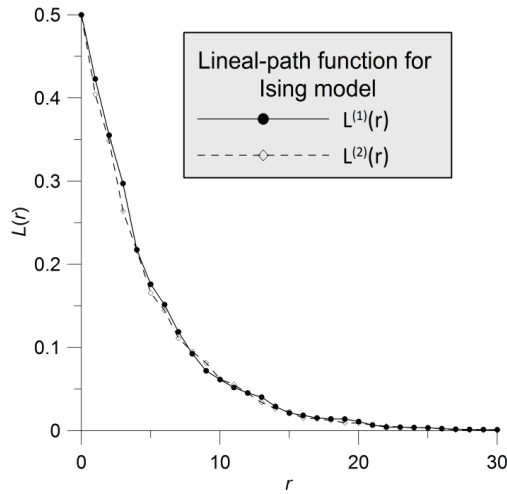versus distance $r$ given in pixels

Fig. 6. Lineal-path function for the Ising model microstructure
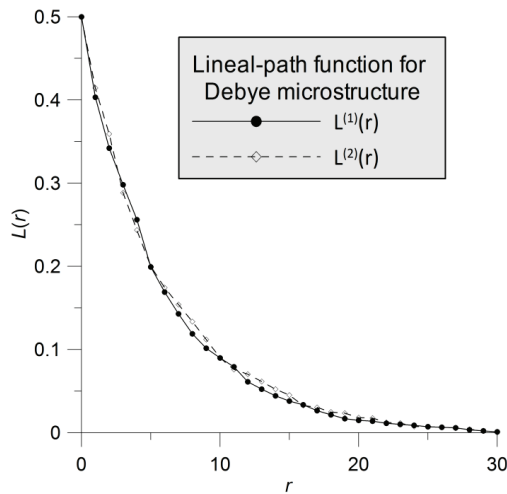versus distance *r* given in pixels



Fig. 7. Lineal-path function for Debye microstructure
versus distance *r* given in pixels

## 4. NUMERICAL EXAMPLES

As mentioned in the Introduction, within the proposed approach (Fig. 1), the primary role is played by the proper evaluation of the RVE size as well as the sample size *n*. The latter is evaluated by the iterative procedure based on the Central Limit Theo-

rem (CLT). Since this problem has been studied in earlier works ([14], [18]), it is not widely discussed in this paper. Furthermore, for more details concerning the CLT, the reader is referred to [2]. It is, however, worth mentioning that the size of the sample $n$ depends mainly on the assumed value of relative error as well as the significance level. In general, according to the CLT, the sample size $n$ is governed by the following inequality [14]

$$n \geq \left(\frac{\sigma}{\mu\varepsilon}\right)^2 \left(\Phi^{-1}\left(1-\frac{\alpha}{2}\right)\right)^2 \tag{11}$$

where $\sigma^2$ and $\mu$ are the variance and expectation of random variable, respectively. Furthermore, $\Phi$ is the cumulative distribution function of the standard normal random variable, $\alpha$ denotes the significance level, and $\varepsilon$ is the relative error of estimation. Note that all the results presented below are obtained with the assumption that $\alpha = 5\%$ and $\varepsilon = 5\%$.

For all three types of microstructures the ensemble average (3) has been calculated for different sizes of $N$. Hence, in each step, the appropriate linear elastic boundary value problem had to be solved. Periodic boundary conditions were prescribed at the peripheries of each $RVE_j$. The summing in relation (3) was stopped each time the inequality (11) had been fulfilled. The convergence of elastic constants as a function of size $N$ is presented in Figs. 8 through 10 for random checkerboard, the Ising model and Debye microstructure, respectively. Moreover, in each plot, the effective elastic constant is also displayed – the dashed line. The effective property was calculated for the large RVE size, i.e., the size of RVE for which only one realization is sufficient.

The error bounds displayed by the dashed-dotted line (Figs. 8–10) require some further explanations. Consider an arbitrary microstructure and assume that the size of RVE is $N < \infty$. Let us denote the mean value of effective elastic constant as $\overline{\lambda}$. Furthermore, the expectation of overall property, for a given size $N < \infty$, is $\lambda_N$. The response for infinite volume – "real" effective property – is $\lambda_\infty$. According to CLT, for the chosen size $N < \infty$, the following inequality should be satisfied

$$(1-\varepsilon)\lambda_N \leq \overline{\lambda} \leq (1+\varepsilon)\lambda_N. \tag{12}$$

On the other hand, the overall response $\lambda_N$ differs from the infinite body result $\lambda_\infty$ in the same manner as relation (12). Therefore, assuming that $\varepsilon^2$ is the higher order negligible term we can express the error bounds as

$$(1-2\varepsilon)\lambda_\infty \leq \overline{\lambda} \leq (1+2\varepsilon)\lambda_\infty. \tag{13}$$
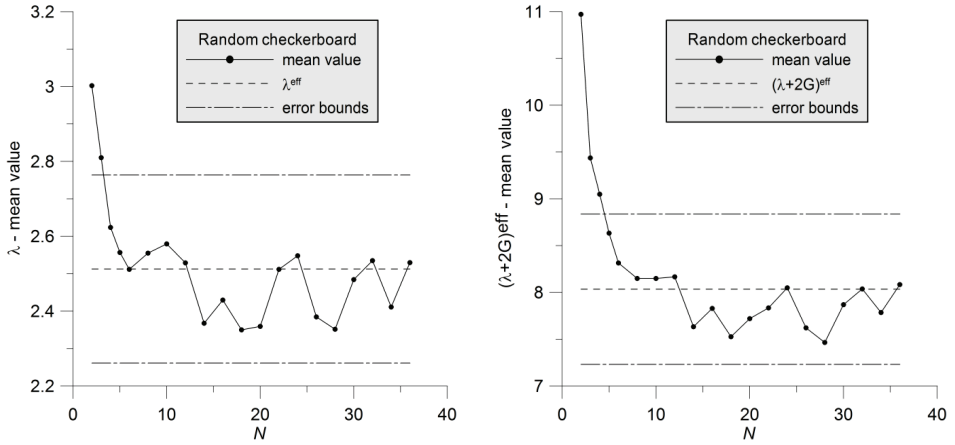
Fig. 8. The convergence of elastic constants with increasing the size of RVE
for random checkerboard; left: mean value of $\lambda$; right: mean value of $(\lambda + 2G)$
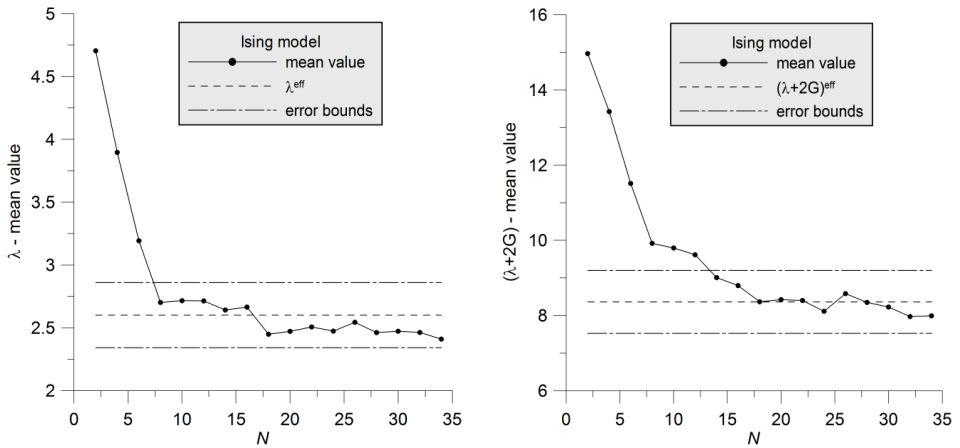


Fig. 9. The convergence of elastic constants with increasing the size of RVE
for the Ising model microstructure; left: mean value of $\lambda$; right: mean value of $(\lambda + 2G)$

The RVE size established by investigating the convergence of elastic constants is determined in the following way. From each convergence plot the minimum size, for which the mean value is between error bounds, is recorded. The minimum size corresponding to $\lambda$ convergence plot is denoted by $N_\lambda$ whereas the one resulting from $(\lambda + 2G)$ plot is $N_{(\lambda+2G)}$. Finally, the size of RVE is expressed as

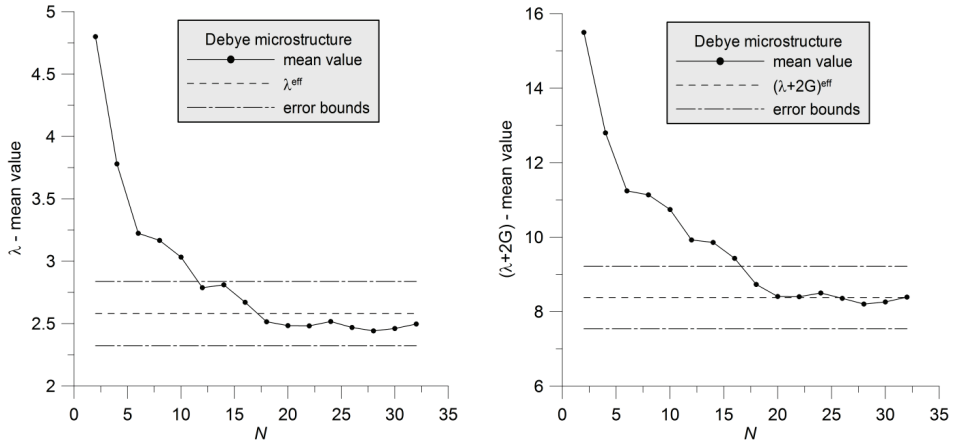$$N_{\mathrm{RVE}} \geq \max\{N_\lambda, N_{(\lambda+2G)}\} . \tag{14}$$

Fig. 10. The convergence of elastic constants with increasing the size of RVE
for Debye microstructure; left: mean value of $\lambda$; right: mean value of $(\lambda + 2G)$

The minimum RVE sizes, i.e., the sizes for which the inequality sign "$\geq$" in (14) is
replaced by "=" are summarized in Table 1.

Table 1

Minimum RVE sizes determined on the basis
of the convergence of the mean value

|  | Random checkerboard | Ising model | Debye microstructure |
|---|---|---|---|
| $N_\lambda$ | 4 | 8 | 12 |
| $N_{(\lambda + 2G)}$ | 5 | 14 | 18 |
| $N_{\mathrm{RVE}}$ | 5 | 14 | 18 |

One can simply notice the largest size of RVE was obtained in the case of Debye
microstructure. On the other hand, the smallest one was established for random check-
erboard. The microstructure reconstructed on the basis of the Ising model exhibits the
size of RVE that is in-between.

What is remarkable, observing the plots of lineal-path functions (Figs. 5–7), is that
the largest lineal-path was also observed for the Debye microstructure, whereas the
shortest one for random checkerboard. The largest lineal-path of the Ising model mi-
crostructure is in-between. Hence, it is quite reasonable to state that there exists some
relation between the largest lineal-path (observed from the "tail" of the lineal-path
function) of a given microstructure and the size of RVE.

Due to the fact that the lineal-path function was determined by making use of
Monte Carlo simulations (10) it is assumed that the largest lineal-path is the value of $r$

for which the following exists

$$\forall r \in [0, \infty] \Rightarrow L^{(i)}(r) \le \varepsilon_{l-p} \qquad (15)$$

where $\varepsilon_{l-p}$ is the error which should be a reasonably small value. The results, i.e., the largest lineal-paths for different values of $\varepsilon_{l-p}$ are presented in Table 2.

Table 2

The largest lineal-path, determined on the basis of (15),
for different values of $\varepsilon_{l-p}$

| Assumed estimation error $\varepsilon_{l-p}$ | The largest lineal-path given in pixels | | |
| --- | --- | --- | --- |
| | Random checkerboard | Ising model | Debye microstructure |
| 5% | 4 | 12 | 16 |
| 3% | 5 | 14 | 18 |
| 1% | 6 | 20 | 24 |

One can simply observe that the largest lineal-paths coincide (in the bounds of numerical error limits) with the size of RVE determined from the convergence of elastic constants. In the case of $\varepsilon_{l-p} = 5\%$, the minimum RVE size is a little bit underestimated, while in the case of $\varepsilon_{l-p} = 1\%$ it is overestimated. For the estimation error $\varepsilon_{l-p} = 3\%$ the largest lineal-path is exactly equal to the minimum RVE size, $N_{\mathrm{RVE}}$ (compare the results in Tables 1 and 2).

## 5. CONCLUSIONS

As previously mentioned it is usually proposed in the literature to determine the size of RVE by investigating the convergence of apparent properties with increasing the size of RVE. Such algorithms usually require a very large number of numerical calculations. In this paper, some numerical studies for the problem of linear elasticity were performed. It was postulated and verified that there exists some direct relation between RVE size and the "tail" of the lineal-path function. Based on the numerical calculations of elastic constants as well as lineal-path functions it was stated that the size of RVE is related to the largest lineal-path of given microstructures.

This paper should be treated as a preliminary study. The validation was performed for only three different two-phase random microstructures having equal volume fraction of constituents. The studies concerned also only one value of the contrast in mechanical properties, i.e., $\lambda_1 : \lambda_2 = G_1 : G_2 = 1 : 10$. As is commonly

known, the RVE size is strongly affected by the volume fraction of constituents as well as the contrast in properties, hence further studies are going to be the subject of our future work.

REFERENCES

[1] BERAN M.J., *Statistical Continuum Theories*, Monographs in Statistical Physics, Interscience Publishers, 1968.

[2] FELLER W., *An Introduction to Probability Theory and its Applications*, Vol. I, 2nd Edition, John Wiley and Sons, N.Y., 1961.

[3] GITMAN I.M., ASKES H., SLUYS L.J., *Representative volume: existence and size determination*, Eng. Fract. Mech., Vol. 74, 2007, 2518–2534.

[4] GRAHAM S., YANG N., *Representative volumes of materials based on microstructural statistics*, Scripta Materialia, Vol. 48, 2003, 269–274.

[5] GRUFMAN C., FERNAND E., *Determining a representative volume element capturing the morphology of fibre reinforced polymer composites*, Compos. Sci. Technol., Vol. 67, 2007, 766–775.

[6] GUSEV A., *Representative volume element size for elastic composites: a numerical study*, J. Mech. Phys. Solids, Vol. 45, 1997, 1449–1459.

[7] JANKE W., *Pseudo random number: generation and quality checks*, Lecture Notes John von Neumann Institute for Computing, Vol. 10, 2002, 447.

[8] KANIT T., FOREST S., GALLIET I., MOUNOURY V., JEULIN D., *Determination of the size of the representative volume element for random composites: statistical and numerical approach*, Int. J. Solids. Struct., Vol. 40, 2003, 3647.

[9] KIRKPATRICK S., GELATT C.D., VECCHI M.P., *Optimization by simulated annealing*, Science, Vol. 220, 1983, 671–680.

[10] LU B., TORQUATO S., *Lineal-path function for random heterogeneous materials*, Phys. Rev. A, 1992, Vol. 45 (2), 922–929.

[11] Mathematica: *Wolfram Mathematica Tutorial Collection*, 2008.

[12] POVIRK G.L., *Incorporation of microstructural information into model of two-phase materials*, Acta Metal. Mater., Vol. 43 (8), 1995, 3199–3206.

[13] QUINTANILLA J., TORQUATO S., *Lineal measures of clustering in overlapping particle systems*, Phys. Rev. E, Vol. 54 (4), 1996, 4027–4036.

[14] RÓŻAŃSKI A., *Random composites: representativity, minimum RVE size, effective transport properties,* PhD dissertation, USTL, LML (UMR CNRS 8107), No. 40444, 2010.

[15] RÓŻAŃSKI A., ŁYDŻBA D., *RVE determination from a digital image of microstructure*, Proceedings of the 2nd Int. Symp. on Comput. Geomech., COMGEO II, S. Pietruszczak et al. (eds.), Rhodes: IC2E International Centre for Computational Engineering, 2011.

[16] RÓŻAŃSKI A., ŁYDŻBA D., *From digital image of microstructure to the size of representative volume element: $B_4C/Al$ composite*, Studia Geotechnica et Mechanica, Vol. XXXIII, No. 1, 2011, 55–68.

[17] RÓŻAŃSKI A., ŁYDŻBA D., SHAO J.F., *Numerical determination of minimum size of RVE for random composite materials: two-point probability approach*, Proceedings of the 1st Int. Symp. on Comput. Geomech., COMGEO I, Juan les Pins, 2009.

[18] RÓŻAŃSKI A., ŁYDŻBA D., SOBÓTKA M., *Numerical determination of effective transport proeprties on the basis of microstructure digital images*, AGH Journal of Mining and Geoengineering, Vol. 34 (2), 2010, 537–552 (in Polish).

[19] SEJNOHA M., ZEMAN J., *Micromechanical Analysis of Random Composites*, Czech Technical Univ., 2000.

[20] STROEVEN M., ASKES H., SLUYS L.J., *Numerical determination of representative volumes for granular materials*, Comput. Methods Appl. Mech. Eng., Vol. 193, 2004, 3221–3238.

[21] TORQUATO S., *Random Heterogeneous Materials. Microstructure and Macroscopic Properties*, Springer-Verlag, New York, 2002.

[22] YEONG C.L.Y., TORQUATO S., *Reconstructing random media*, Phys. Rev. E, Vol. 587, 1998, 495.

[23] YEONG C.L.Y., TORQUATO S., *Reconstructing random media. II. Three-dimensional media form two-dimensional cuts,* Phys. Rev. E, Vol. 58, 1998, 224.

[24] ZEMAN J., SEJNOHA M., *Numerical evaluation of effective elastic properties of graphite fiber tow impregnated by polymer matrix*, J. Mech. Phys. Solids, Vol. 49, 2001, 69.